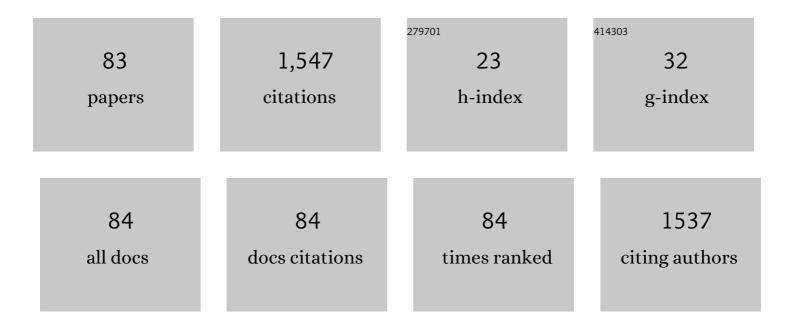
List of Publications by Year in descending order

Source: https://exaly.com/author-pdf/208405/publications.pdf Version: 2024-02-01



MALTHANH NOUVEN

#	Article	IF	CITATIONS
1	Chemical synthesis of blue-emitting metallic zinc nano-hexagons. CrystEngComm, 2013, 15, 6606.	1.3	86
2	Sputtering onto a liquid: interesting physical preparation method for multi-metallic nanoparticles. Science and Technology of Advanced Materials, 2018, 19, 883-898.	2.8	61
3	Low temperature sintering process of copper fine particles under nitrogen gas flow with Cu <sup>2+</sup> -alkanolamine metallacycle compounds for electrically conductive layer formation. RSC Advances, 2016, 6, 12048-12052.	1.7	55
4	Binder-Free Centimeter-Long V2O5 Nanofibers on Carbon Cloth as Cathode Material for Zinc-Ion Batteries. Energies, 2020, 13, 31.	1.6	43
5	Porous ZnV <sub>2</sub> O <sub>4</sub> Nanowire for Stable and High-Rate Lithium-Ion Battery Anodes. ACS Applied Nano Materials, 2019, 2, 4247-4256.	2.4	41
6	A new approach for additive-free room temperature sintering of conductive patterns using polymer-stabilized Sn nanoparticles. Journal of Materials Chemistry C, 2016, 4, 2228-2234.	2.7	40
7	Annealing induced a well-ordered single crystal Î-MnO2 and its electrochemical performance in zinc-ion battery. Scientific Reports, 2019, 9, 15107.	1.6	37
8	MnO2 Heterostructure on Carbon Nanotubes as Cathode Material for Aqueous Zinc-Ion Batteries. International Journal of Molecular Sciences, 2020, 21, 4689.	1.8	37
9	Enhanced Cycling Performance of Rechargeable Zinc–Air Flow Batteries Using Potassium Persulfate as Electrolyte Additive. International Journal of Molecular Sciences, 2020, 21, 7303.	1.8	36
10	Microwave-Induced Plasma-In-Liquid Process for Nanoparticle Production. Bulletin of the Chemical Society of Japan, 2018, 91, 1781-1798.	2.0	35
11	Benchmarking superfast electrodeposited bimetallic (Ni, Fe, Co, and Cu) hydroxides for oxygen evolution reaction. Journal of Alloys and Compounds, 2021, 889, 161738.	2.8	35
12	Au/Cu Bimetallic Nanoparticles via Double-Target Sputtering onto a Liquid Polymer. Langmuir, 2017, 33, 12389-12397.	1.6	33
13	Synthesis of Positively Charged Photoluminescent Bimetallic Au–Ag Nanoclusters by Double-Target Sputtering Method on a Biocompatible Polymer Matrix. Langmuir, 2017, 33, 9144-9150.	1.6	33
14	β-Sn Nanorods with Active (001) Tip Induced LiF-Rich SEI Layer for Stable Anode Material in Lithium Ion Battery. ACS Applied Nano Materials, 2018, 1, 3509-3519.	2.4	32
15	Silver Decorated Reduced Graphene Oxide as Electrocatalyst for Zinc–Air Batteries. Energies, 2020, 13, 462.	1.6	32
16	Preparation of Au/Pd Bimetallic Nanoparticles by a Microwave-Induced Plasma in Liquid Process. Bulletin of the Chemical Society of Japan, 2017, 90, 279-285.	2.0	31
17	Double target sputtering into liquid: A new approach for preparation of Ag–Au alloy nanoparticles. Materials Letters, 2016, 171, 75-78.	1.3	30
18	Effect of decomposition and organic residues on resistivity of copper films fabricated via low-temperature sintering of complex particle mixed dispersions. Scientific Reports, 2017, 7, 45150.	1.6	28

#	Article	IF	CITATIONS
19	Use of decomposable polymer-coated submicron Cu particles with effective additive for production of highly conductive Cu films at low sintering temperature. Journal of Materials Chemistry C, 2017, 5, 1033-1041.	2.7	27
20	High-Capacity Dual-Electrolyte Aluminum–Air Battery with Circulating Methanol Anolyte. Energies, 2020, 13, 2275.	1.6	27
21	A durable rechargeable zinc-air battery via self-supported MnOx-S air electrode. Journal of Alloys and Compounds, 2021, 883, 160935.	2.8	27
22	Size-Tunable Alumina-Encapsulated Sn-Based Phase Change Materials for Thermal Energy Storage. ACS Applied Nano Materials, 2019, 2, 3752-3760.	2.4	26
23	Stabilization of the thermal decomposition process of self-reducible copper ion ink for direct printed conductive patterns. RSC Advances, 2017, 7, 25095-25100.	1.7	25
24	ZnV2O4: A potential anode material for sodium-ion batteries. Journal of the Taiwan Institute of Chemical Engineers, 2018, 88, 161-168.	2.7	25
25	Au Nanoplasma as Efficient Hard X-ray Emission Source. ACS Photonics, 2016, 3, 2184-2190.	3.2	24
26	Recent advances in oxygen electrocatalysts based on tunable structural polymers. Materials Today Chemistry, 2022, 23, 100632.	1.7	24
27	Electrochemical properties of novel FeV2O4 as an anode for Na-ion batteries. Scientific Reports, 2018, 8, 8839.	1.6	22
28	Electrochemical exploration of the effects of calcination temperature of a mesoporous zinc vanadate anode material on the performance of Na-ion batteries. Inorganic Chemistry Frontiers, 2019, 6, 2653-2659.	3.0	22
29	Binder-Free α-MnO2 Nanowires on Carbon Cloth as Cathode Material for Zinc-Ion Batteries. International Journal of Molecular Sciences, 2020, 21, 3113.	1.8	22
30	Micro- and nano-encapsulated metal and alloy-based phase-change materials for thermal energy storage. Nanoscale Advances, 2021, 3, 4626-4645.	2.2	21
31	Synthesis of magnetic mesoporous titania colloidal crystals through evaporation induced self-assembly in emulsion as effective and recyclable photocatalysts. Physical Chemistry Chemical Physics, 2015, 17, 27653-27657.	1.3	20
32	Bismuth, antimony and tellurium alloy nanoparticles with controllable shape and composition for efficient thermoelectric devices. Physica Status Solidi (A) Applications and Materials Science, 2011, 208, 52-58.	0.8	19
33	Sub-2 nm Single-Crystal Pt Nanoparticles via Sputtering onto a Liquid Polymer. Langmuir, 2018, 34, 2876-2881.	1.6	19
34	High Aspect Ratio and Post-Processing Free Silver Nanowires as Top Electrodes for Inverted-Structured Photodiodes. ACS Omega, 2019, 4, 13303-13308.	1.6	18
35	Au Nanoparticles Prepared Using a Coated Electrode in Plasma-in-Liquid Process: Effect of the Solution pH. Journal of Nanoscience and Nanotechnology, 2016, 16, 9257-9262.	0.9	17
36	Effect of H2O2 on Au nanoparticle preparation using microwave-induced plasma in liquid. Materials Chemistry and Physics, 2017, 193, 7-12.	2.0	17

#	Article	IF	CITATIONS
37	Synthesis of Au@Cu <sub>2</sub> O Core–Shell Nanoparticles with Tunable Shell Thickness and Their Degradation Mechanism in Aqueous Solutions. Langmuir, 2020, 36, 3386-3392.	1.6	17
38	Matrix Sputtering into Liquid Mercaptan: From Blue-Emitting Copper Nanoclusters to Red-Emitting Copper Sulfide Nanoclusters. Langmuir, 2016, 32, 12159-12165.	1.6	16
39	Highly Correlated Size and Composition of Pt/Au Alloy Nanoparticles via Magnetron Sputtering onto Liquid. Langmuir, 2020, 36, 3004-3015.	1.6	16
40	Preparation and Growth Mechanism of Pt/Cu Alloy Nanoparticles by Sputter Deposition onto a Liquid Polymer. Langmuir, 2019, 35, 8418-8427.	1.6	15
41	Synergistic Effect of the Oleic Acid and Oleylamine Mixed-Liquid Matrix on Particle Size and Stability of Sputtered Metal Nanoparticles. ACS Sustainable Chemistry and Engineering, 2020, 8, 18167-18176.	3.2	15
42	Study on formation mechanism and ligand-directed architectural control of nanoparticles composed of Bi, Sb and Te: towards one-pot synthesis of ternary (Bi,Sb)2Te3 nanobuilding blocks. RSC Advances, 2011, 1, 1089.	1.7	14
43	Ball mill-assisted synthesis of NiFeCo-NC as bifunctional oxygen electrocatalysts for rechargeable zinc-air batteries. Journal of Alloys and Compounds, 2022, 922, 166287.	2.8	14
44	Cladding Layer on Well-Defined Double-Wall TiO <sub>2</sub> Nanotubes. Langmuir, 2015, 31, 1575-1580.	1.6	13
45	Highly stable and blue-emitting copper nanocluster dispersion prepared by magnetron sputtering over liquid polymer matrix. RSC Advances, 2016, 6, 105030-105034.	1.7	13
46	Structural Control Parameters for Formation of Single-Crystalline β-Sn Nanorods in Organic Phase. Crystal Growth and Design, 2017, 17, 4554-4562.	1.4	13
47	Ligand free green plasma-in-liquid synthesis of Au/Ag alloy nanoparticles. New Journal of Chemistry, 2018, 42, 5680-5687.	1.4	13
48	Ethylene Glycol/Ethanol Anolyte for High Capacity Alkaline Aluminum-Air Battery With Dual-Electrolyte Configuration. Frontiers in Energy Research, 2020, 8, .	1.2	13
49	Control of nanoparticles synthesized <i>via</i> vacuum sputter deposition onto liquids: a review. Soft Matter, 2021, 18, 19-47.	1.2	13
50	Proton-assisted low-temperature sintering of Cu fine particles stabilized by a proton-initiating degradable polymer. RSC Advances, 2015, 5, 102904-102910.	1.7	12
51	<scp>l</scp> -Arginine-Stabilized Highly Uniform Ag Nanoparticles Prepared in a Microwave-Induced Plasma-in-Liquid Process (MWPLP). Bulletin of the Chemical Society of Japan, 2018, 91, 362-367.	2.0	12
52	Green Synthesis of Size-Tunable Iron Oxides and Iron Nanoparticles in a Salt Matrix. ACS Sustainable Chemistry and Engineering, 2019, 7, 17697-17705.	3.2	12
53	Efficient iron–cobalt oxide bifunctional electrode catalysts in rechargeable high current density zinc–air batteries. Nanoscale, 2022, 14, 8012-8022.	2.8	12
54	Femtosecond laser-induced hard X-ray generation in air from a solution flow of Au nano-sphere suspension using an automatic positioning system. Optics Express, 2016, 24, 19994.	1.7	11

#	Article	IF	CITATIONS
55	Titanium oxide nanoparticle dispersions in a liquid monomer and solid polymer resins prepared by sputtering. New Journal of Chemistry, 2016, 40, 9337-9343.	1.4	11
56	Sn Nanoparticles Confined in Porous Silica Spheres for Enhanced Thermal Cyclic Stability. ACS Applied Nano Materials, 2018, 1, 4073-4082.	2.4	11
57	Effects of Additives on the Preparation of Ag Nanoparticles Using the Microwaveâ€Induced Plasma in Liquid Process. ChemistrySelect, 2017, 2, 7873-7879.	0.7	10
58	Surfactant-stabilized copper paticles for low-temperature sintering: Paste preparation using a milling with small zirconia beads: Effect of pre-treatment with the disperse medium. Advanced Powder Technology, 2020, 31, 4570-4575.	2.0	10
59	Elucidation of the Complex Structure of Nanoparticles Composed of Bismuth, Antimony, and Tellurium Using Scanning Transmission Electron Microscopy. Journal of Physical Chemistry C, 2011, 115, 17334-17340.	1.5	9
60	Synthesis of composition-tunable Pd–Cu alloy nanoparticles by double target sputtering. New Journal of Chemistry, 2020, 44, 4704-4712.	1.4	9
61	Synthesis and fluorescence properties of a nanoisland-structured SiO <sub>x</sub> /Cu <sub>x</sub> O composite. Journal of Materials Chemistry C, 2015, 3, 8358-8363.	2.7	8
62	One-pot Chemical Synthesis of Zinc Antimonide Nanoparticles as Building Blocks for Nanostructured Thermoelectric Materials. Chemistry Letters, 2012, 41, 1529-1531.	0.7	7
63	MHz-ultrasound generation by chirped femtosecond laser pulses from gold nano-colloidal suspensions. Optics Express, 2016, 24, 17050.	1.7	7
64	Reproducible shape control of single-crystal SnO micro particles. RSC Advances, 2016, 6, 26725-26733.	1.7	7
65	Particle size tuning in scalable synthesis of anti-oxidized copper fine particles by polypeptide molecular weights. Advanced Powder Technology, 2017, 28, 1966-1971.	2.0	7
66	Synthesis of Sn/Ag–Sn nanoparticles via room temperature galvanic reaction and diffusion. RSC Advances, 2019, 9, 21786-21792.	1.7	7
67	Monitor the Growth and Oxidation of Cu-nanoparticles in PEG after Sputtering. MRS Advances, 2019, 4, 305-309.	0.5	7
68	Pt/Ag Solid Solution Alloy Nanoparticles in Miscibility Gaps Synthesized by Cosputtering onto Liquid Polymers. Langmuir, 2021, 37, 6096-6105.	1.6	7
69	Copper Materials for Low Temperature Sintering. Materials Transactions, 2022, 63, 663-675.	0.4	7
70	Impact of Morphology and Transition Metal Doping of Vanadate Nanowires without Surface Modification on the Performance of Aqueous Zinc-Ion Batteries. Bulletin of the Chemical Society of Japan, 2022, 95, 728-734.	2.0	7
71	The role of surface oxides and stabilising carboxylic acids of copper nanoparticles during low-temperature sintering. Materials Advances, 2022, 3, 4802-4812.	2.6	6
72	CoxNi1-xO-NiCo2O4/rGO Synergistic Bifunctional Electrocatalysts for High-Rate Rechargeable Zinc-Air Battery. Sustainable Energy and Fuels, 0, , .	2.5	6

#	Article	IF	CITATIONS
73	Enhanced Terahertz Emission from Cu <i>x</i> O/Metal Thin Film Deposited on Columnar-Structured Porous Silicon. Bulletin of the Chemical Society of Japan, 2015, 88, 1385-1387.	2.0	5
74	Mesoporous Europium-Doped Titania Nanoparticles (Eu-MTNs) for Luminescence-Based Intracellular Bio-Imaging. Journal of Nanoscience and Nanotechnology, 2015, 15, 9802-9806.	0.9	5
75	Alginate-Stabilized Gold Nanoparticles Prepared Using the Microwave-Induced Plasma-in-Liquid Process with Long-Term Storage Stability for Potential Biomedical Applications. ACS Omega, 2022, 7, 6238-6247.	1.6	5
76	Size-controlled Preparation of Alkylamine-stabilized Copper Fine Particles from Cupric Oxide (CuO) Micro-particles. MRS Advances, 2019, 4, 413-418.	0.5	4
77	THz wave emission from the Cu <sub>2</sub> O/Cu interface under femtosecond laser irradiation. Applied Physics Express, 2021, 14, 012006.	1.1	3
78	Preparation of Biopex-Supported Gold Nanoparticles as Potential Fiducial Markers for Image-Guided Radiation Therapy. ACS Applied Bio Materials, 2022, 5, 1259-1266.	2.3	3
79	Chemical Synthesis of Binary Solid Solution Bismuth–Antimony Nanoparticles with Control of Composition and Morphology. Chemistry Letters, 2014, 43, 615-617.	0.7	2
80	THz Wave Emission from ZnTe Nano-colloidal Aqueous Dispersion Irradiated by Femtosecond Laser. Chemistry Letters, 2020, 49, 597-600.	0.7	2
81	In situ TEM observation of liquid-state Sn nanoparticles vanishing in a SiO2 structure: a potential synthetic tool for controllable morphology evolution from core–shell to yolk–shell and hollow structures. Nanoscale Advances, 2020, 2, 1456-1464.	2.2	2
82	Green and effective synthesis of gold nanoparticles as injectable fiducial marker for real-time image gated proton therapy. Materials Advances, 0, , .	2.6	2
83	Anisotropic Growth of Copper Nanorods Mediated by Cl <sup>–</sup> Ions. ACS Omega, 2022, 7, 7414-7420.	1.6	Ο